Journal of Applied Mechanics and Technical Physics, Vol. 49, No. 5, pp. 770–775, 2008

DEFORMATION BOUNDARIES OF AN AXISYMMETRIC CAVITY BY GAS JETS

A. N. Varyukhin

UDC 532.528, 532.522.2

A method is proposed for calculating small deformations of the boundaries of an axisymmetric cavity with impinging gas jets. No constraints are imposed on the configuration and characteristics of the system of nozzles generating the jets. Numerical results are compared with data obtained by available semi-empirical methods and with experimental data.

Key words: *supercavitation, geometry of slender cavities, gas jets, impinging of gas jets on targets.*

Introduction. Cavitation cavities are usually created by the method of gas injection with the formation of the so-called ventilated cavities. For the cavity geometry to be free from distortions, the gas is injected directly behind the cavitator with extremely small velocities. It is rather difficult, however, to satisfy these conditions in practice; high-pressure gas jets generate an excess pressure field on the cavity boundaries, which inevitably leads to deformation of these boundaries.

Zhuravlev [1] considered the problem of small deformations of a slender axisymmetric cavity under the action of various factors, for instance, excess pressure on the liquid boundaries. The pressure distribution necessary for finding the strains has to be determined by another method, for example, from experiments. Zhuravlev and Romanovskii [2] calculated the shape of the cavity with a subsonic circular jet impinging on the cavity boundary; the pressure distribution was taken from an experiment on jet interaction with a flat target. Such a method, however, where labor-consuming experiments are combined with an uncertain error in calculating the perturbations of liquid boundaries, is not perfect.

The objective of the present work is to develop a method for calculating the cavity shape with gas jets present inside the cavity without using any experimental data. For this purpose, we have to formulate a hydrogasdynamic problem where the gas flow in the cavity and the liquid flow outside the cavity are interrelated phenomena. This problem is solved with the use of equations [1] for small deformations of the cavity boundary and the Navier–Stokes equations for the gas flow inside the deformed cavity.

Formulation of the Problem. Let a cavitator move with a constant velocity in an unconfined, inviscid, and incompressible liquid, and let a slender axisymmetric cavity with a constant pressure on the boundary be formed behind the cavitator. The slenderness of such a cavity (which will be called the unperturbed cavity) is $\varepsilon = R_k/L_k \ll 1$ (R_k is the cavity radius and L_k is the cavity half-length). The cavity shape $r = R_0(x)$ is assumed to be known (Fig. 1).

We put an arbitrary system of nozzles generating gas jets into the unperturbed cavity. Then, an additional pressure field $\Delta p(x,\theta)$ is generated on the liquid boundaries [additional cavitation number $\Delta\sigma = -\Delta p/(\rho V_0^2/2)$, where V_0 is the cavitator velocity], which results in deformation of the initial shape of the cavity.

We have to find the shape of the deformed cavity $R(x,\theta) = R_0(x) + \eta(x,\theta)$, where $\eta(x,\theta)$ is the deformation of the liquid boundaries caused by the excess pressure $\Delta p(x,\theta)$. The coordinate system is shown in Fig. 1. The gas flow is assumed to obey the Navier–Stokes equations. The values of deformations $\eta(x,\theta)$ are determined by the joint solution of the Euler equations (for the liquid) and Navier–Stokes equations (for the gas) under the condition

Department of the Joukowski Central Aerohydrodynamic Institute "Moscow Department of TsAGI," Moscow 105005; bosporecz@gmail.com. Translated from Prikladnaya Mekhanika i Tekhnicheskaya Fizika, Vol. 49, No. 5, pp. 80–86, September–October, 2008. Original article submitted October 8, 2007.

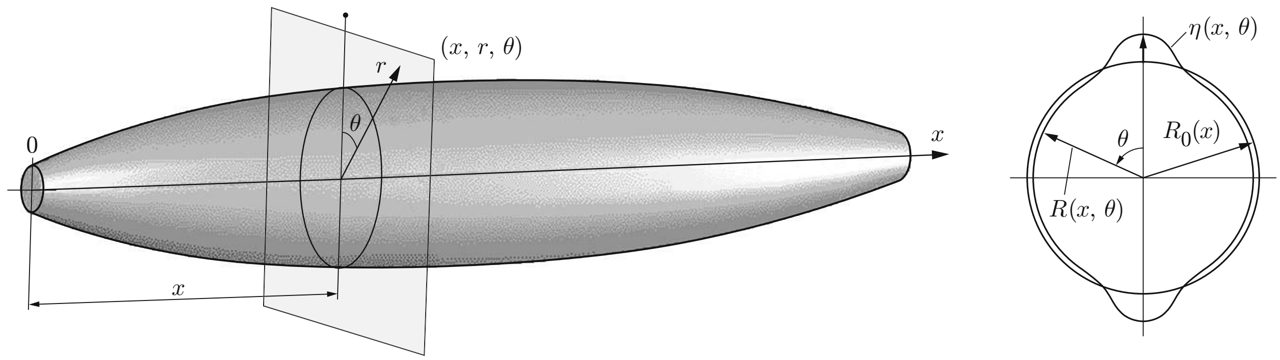

Fig. 1. Schematic of the cavity and coordinate system.

of identical static pressures and shear and normal velocities on the liquid–gas interface and with allowance for the influence of the heat flux on the liquid boundary.

In deriving the equations of small deformations of a slender axisymmetric cavity with the use of the smallness parameter $\delta = \eta/R_0 \ll 1$, Zhuravlev [1] obtained an infinite system of linear equations with respect to the coefficients of decomposition of strains into a Fourier series. For the problem considered with accuracy to $\varepsilon\delta$, this system has the form

$$R_0\eta_0'' + 2R_0'\eta_0' + R_0''\eta_0 = -(k/2)\Delta\sigma_0, \qquad j = 0,$$
$$R_0\eta_j'' + 2R_0'\eta_j' - (j-1)R_0''\eta_j = -(j/2)\Delta\sigma_j, \qquad j > 0, \tag{1}$$

where the prime denotes differentiation with respect to the longitudinal coordinate x, the coefficient is $k = 0.55$, and η_j and $\Delta\sigma_j$ are the coefficients of expansion of η and $\Delta\sigma$ into a Fourier series on the interval $[0, 2\pi]$:

$$\Delta\sigma(x,\theta) = \sum_0^\infty \Delta\sigma_j(x)\cos j\theta, \qquad \eta(x,\theta) = \sum_0^\infty \eta_j(x)\cos j\theta.$$

All quantities in the equations are dimensionless. An arbitrary characteristic quantity, for instance, the disk-cavitator radius R_n can be chosen as the linear scale for system (1).

Let us cite the approximate dependences of the geometric parameters of a slender unperturbed cavity from [3, 4]. The equation for the unperturbed cavity has the form

$$R_0(x) = (1+3x)^{1/3}, \quad x < 2, \qquad R_0^2(x) = 0.366 + 0.89(x-2) - \sigma(x-2)^2/4, \quad x \geqslant 2,$$

the mid-section radius of such a cavity is $R_k = R_n\sqrt{C_x(1+\sigma)/\sigma}$, and the half-length of the cavity is $L_k \approx 1.84R_n/\sigma$.

To solve system (1), one has to know the pressure distribution $\Delta\sigma(x,\theta)$ over the cavity surface, which depends on a particular implementation of the injection system and is a function of many parameters in the general case.

Zhuravlev and Romanovskii [2] used the pressure distribution measured in an experiment where a circular axisymmetric jet impinged onto a flat target. The excess pressure perturbing the cavity was assumed to be concentrated within a small interval $\Delta x \ll L_k$.

In the present work, the pressure distribution on the cavity boundary is found by solving numerically a system of the Navier–Stokes equations, more exactly, a system of the Reynolds equations with the k–e model of turbulence for determining the gas flow field inside the cavity.

Method of Calculating the Shape of a Non-Axisymmetric Cavity. As the gas flow field structure inside the cavity strongly depends on the cavity geometry, we used an approach where the boundary of the computational domain and, hence, the computational grid are reconstructed in the course of integration of the equations, and the shape of the computational domain boundary is tuned to the pressure distribution. The essence of this approach implies that: 1) the cavity boundary is assumed to be impermeable for the gas, which means identical normal and tangential velocities of the gas and liquid on the cavity boundary; 2) a heat flux providing an isothermal flow in the rear part of the cavity is set on the computational domain boundary corresponding to the cavity surface [5]; 3) the gas flow inside the cavity is determined by integrating the Navier–Stokes equations with respect to time;

4) at a certain step of solving the gas-flow equations, system (1) is solved with the use of the pressure distribution obtained and a new shape of the cavity is found; after a certain number of time steps, the shape of the computational domain is deformed, and further calculations are performed until the cavity shape becomes stabilized.

The gas flow was computed at the Moscow Institute of Physics and Technology with the use of the ANSYS CFX 10.0 software (license ANSYS 367402). This software system allows the computational domain boundaries to be deformed in accordance with the law defined by user's subroutine developed for solving the problem of deformation of the computational domain boundary. In the course of the computation, the values of the static pressure at each node of the grid on the domain boundary are transferred to the subroutine, and the latter defines new coordinates of nodes of the surface grid. After that, a computational cycle is performed, and the procedure is repeated.

In the course of subroutine operation, the values of pressure are interpolated to a uniform computational grid consisting of N_x elements along the cavity axis and $2N_p$ elements over the angular coordinate. The values of pressure are set at the element centers. Based on a finite-difference relation derived from Eqs. (1), we find the components of the Fourier series of small perturbations

$$\eta_{jk} = \frac{-j\Delta x^2 \Delta\sigma_{jk}/2 + 2R_{0k-1}\eta_{jk-1} - R_{0k-2}\eta_{jk-2}}{(1-j)R_{0k} + 2jR_{0k-1} - jR_{0k-2}},$$

$$k = 1, \ldots, Nx, \qquad j = ni, \qquad i = 1, 2, 3, \ldots \,.$$

Here $\Delta x = (x_{\max} - x_0)/N_x$ is the length of the interval of the uniform grid in the direction of the cavity axis, $R_{0k} = R_0(x_k)$ is the reduced radius of the unperturbed cavity in the cross section with the coordinate $x_k = \Delta xk$, and $\eta_{jk} = \eta_j(x_k)$ is the jth component of the Fourier series of the perturbation of the cavity cross section with the coordinate x_k. The computations performed and the comparison with the experimental data [2] show that it suffices to use the first 10 terms of series (1).

After that, the solution obtained for $R_0(x_k)$ and $\eta_j(x_k)$ on a uniform grid is interpolated to the grid nodes where the pressure values are specified. The deviation of each node from the initial position is calculated, and this value is transferred to the clipboard for data exchange between the ANSYS CFX solver and the subroutine.

Based on the specified displacements of the nodes on the computational domain boundary, the CFX solver deforms the computational grid in the domain, and the fields of gas-dynamic quantities obtained at the previous time step are interpolated to the grid.

The computation also includes the change in the volume of the computational domain. This quantity is used as a criterion of solution convergence. Additional boundary conditions are imposed: 1) zero velocity is set on the body and nozzle surfaces (no-slip conditions); 2) mass flow and stagnation temperature of the gas are set at the nozzle entrance; 3) static pressure is set at the domain exit (rear side of the cavity). The static pressure in the latter case is determined by the semi-empirical expression [5]

$$\frac{G_\Sigma}{\rho_n} = KV_0\pi R_n^2 \, \frac{C_x(1+\sigma)}{\sigma}\Big(1 - \frac{\sigma}{\mathrm{Eu}}\Big),$$

where $K \approx 0.35$ is an empirical coefficient, ρ_n is the gas density under standard conditions, G_Σ is the mass flow of the gas passing through the cavity mid-section, and Eu is the Euler number.

Computation Results and Comparisons with Experiments. To verify the validity of the chosen approach, we performed computations for the case described in [2], for which experimental data and results calculated by a semi-empirical approach are available.

Figure 2 shows a schematic view of the experimental setup. An axisymmetric cavity is formed with the help of air injection with the cavitator moving in water. Two nozzles are mounted symmetrically inside the cavity perpendicular to its axis. These nozzle issue air jets deforming the cavity.

The following data are used in the computation: velocity of cavitator motion $V_0 = 8$ m/sec, disk-cavitator radius $R_n = 13$ mm, cavitation number of the unperturbed cavity $\sigma = 0.0432$, nozzle diameter $d_{\mathrm{noz}} = 5$ mm, distance between the cavitator and the center of the nozzle-exit section along the cavity axis $x_{\mathrm{noz}} = 208$ mm, pressure at the depth of motion $P_h = 105,500$ Pa, stagnation temperature of injected air and air escaping from the nozzles $T_0 = 288$ K, mass flow rate of the injected gas $G = 0.035$ kg/sec, which corresponds to the volume mass flow $Q = 0.027$ m^3/sec under standard conditions, and specific impulse of the injected jet $\bar{J} = J/(C_x\pi R_n^2\rho V_0^2/2) \approx 0.2$.

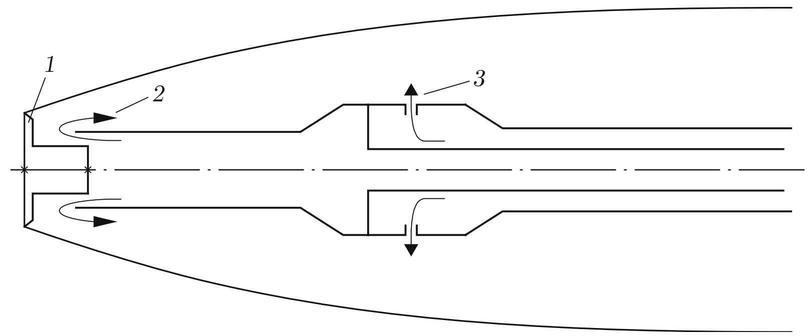

Fig. 2. Experimental setup: 1) cavitator; 2) injection; 3) nozzle.

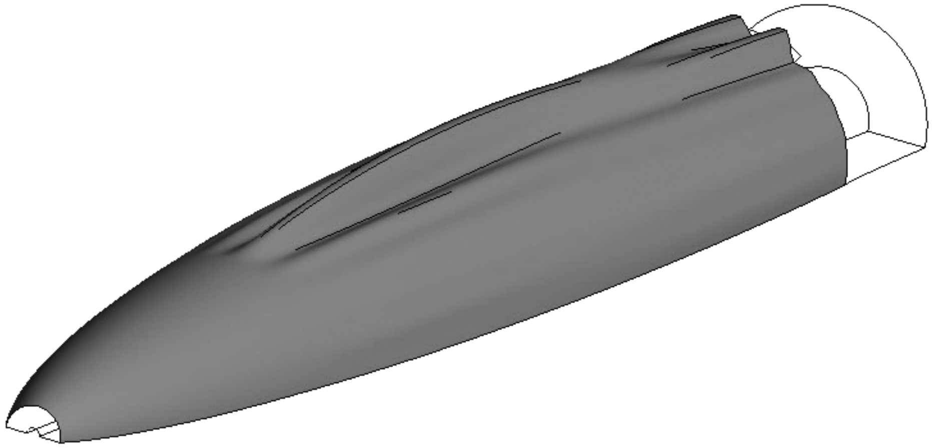

Fig. 3. Computed cavity shape.

A series of computations with different specific impulses of the jet was performed. The results presented below refer to the impulse of the jet exhausting from the nozzle $J_{\text{noz}} = 0.48$ N, which corresponds to the mass flow rate of the gas $G = 0.00347$ kg/sec.

In solving this problem, the heat flux on the computational domain boundary corresponding to the cavity surface was set equal to zero, because the stagnation temperature of the gas ahead of the nozzle equals the liquid temperature and the maximum velocity of the gas flow corresponds to a Mach number M $= 0.3$, i.e., the gas flow is almost isothermal. The computational domain was produced by the SolidWorks 2005 software system, and the computational grid was generated by the ANSYS ICEM CFD 10.0 software system. A structured hexagonal grid was used in computations. By virtue of the problem symmetry, the computational domain included only one half of the cavity.

In this problem, the quality of resolution of the boundary layer by the computational grid was found to exert only a weak effect on the main flow and cavity shape. The height of the first cell in the boundary layer on the basic segment of the boundary is $\Delta y_1 = 0.05$ mm, and the cell height on the nozzle surface is $\Delta y_1 = 0.01$ mm. The computations predict that $y^+ = \Delta y_1/l_\tau \leqslant 50$ on the body surface and $y^+ = \Delta y_1/l_\tau \leqslant 10$ on the nozzle walls (l_τ is the characteristic viscous scale). The computational domain consisted of 457,000 elements.

The flow was calculated in two stages. The first stage included the definition of the initial shape of the cavity boundary, which was not deformed in the course of the gas-flow computation. At the next stage, this solution was used as the initial approximation, and the computation for the deformed boundary was performed.

The equations were integrated with respect to time by an implicit second-order scheme with a step $\Delta t =$ 0.0001 sec, and the mean Courant number averaged over the domain was smaller than 10. Five internal iterations were performed at each step. A second-order total variation diminishing (TVD) scheme was used for approximation of spatial variables.

Figure 3 shows the calculated shape of the half of the cavity deformed by gas jets.

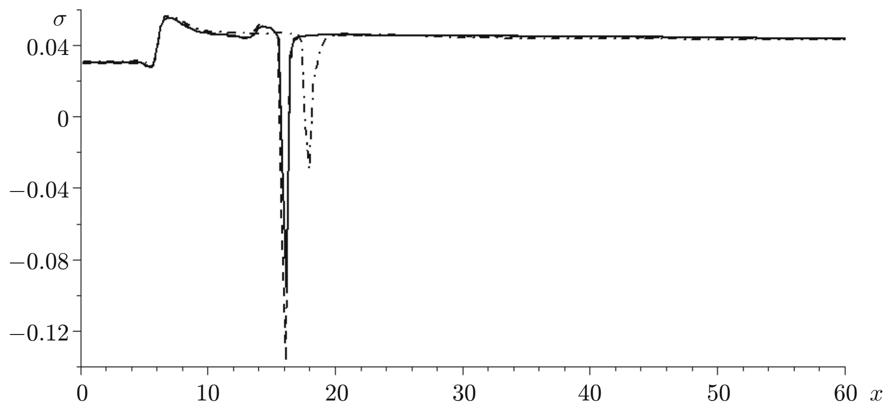

Fig. 4. Distribution of the cavitation number over the cavity surface in the cross section by the plane of symmetry for $J_{\rm noz} = 0.34$ N and $\alpha = 90°$ (solid curve), $J_{\rm noz} = 0.48$ N and $\alpha = 90°$ (dashed curve), and $J_{\rm noz} = 0.48$ N and $\alpha = 45°$ (dot-and-dashed curve).

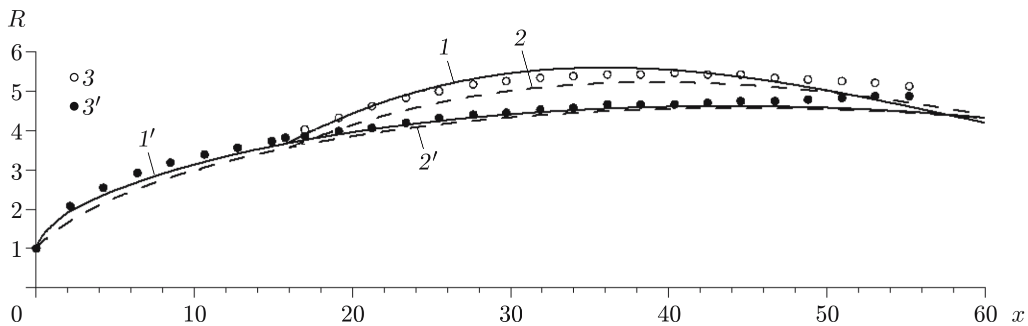

Fig. 5. Profiles of the perturbed cavity (1–3) and unperturbed cavity (1′–3′) in the cross section by the plane of symmetry ($J_{\rm noz} = 0.48$ N and $\alpha = 90°$): curves 1 and 1′ show the results of the numerical calculation, curves 2 and 2′ are the calculations performed in [2], and curves 3 and 3′ are the experimental results [2].

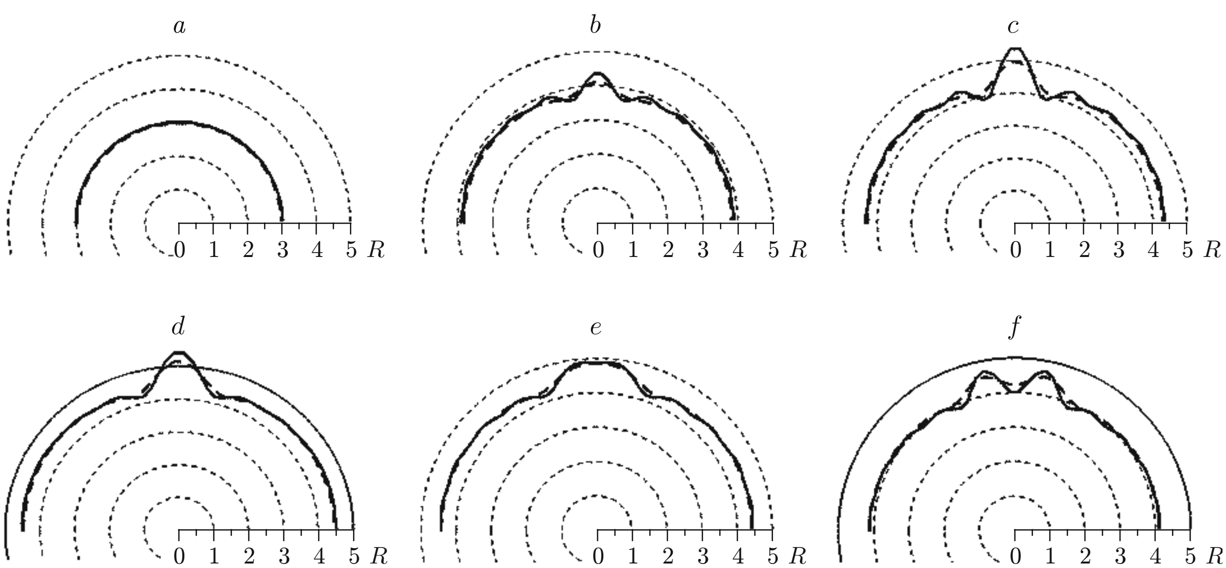

Fig. 6. Cross-sectional profiles of the cavity for $x = 10$ (a), 20 (b), 30 (c), 40 (d), 50 (e), and 60 (f); the solid and dashed curves are the numerical calculations and the calculations performed in [2], respectively.

The distribution of the cavitation number over the cavity surface in the cross section by the plane of symmetry (α is the angle of nozzle alignment) is plotted in Fig. 4. This distribution is seen to have a peaked dip at the point of jet impingement. At the point of impingement of the injected jet in the frontal part, the cavitation number is smaller (hence, the pressure is higher) than on the major part of the cavity.

Figure 5 shows the profiles of the perturbed and unperturbed cavities in the plane of symmetry, which were obtained in [2] and in the present work. Some difference in the profiles in the rear part of the cavity may be caused by cavity buoyancy, because the experiment was performed with comparatively moderate Froude numbers.

The cavity profiles in several cross sections obtained in the present work and in [2] are plotted in Fig. 6. The differences are within the error accepted in deriving Eqs. (1).

Conclusions. A method is developed for calculating the shape of a ventilated cavity modeled by a wall with conditions of no penetration through the wall. The shape of the wall depends on the pressure distribution determined by the joint solution of system (1) and equations for the gas flow inside the cavity. In the course of computations, the computational domain is reconstructed so that the cavity shape corresponds to the pressure distribution computed at the previous step, after which the flow field is again computed. A comparison of the results obtained with available experimental and numerical data show their good agreement.

The method developed allows studying the effect of the nozzle position and configuration and the properties and parameters of the injected gas on the cavity shape.

REFERENCES

1. Yu. F. Zhuravlev, "Methods of the theory of perturbations in spatial jet flows," *Tr. TsAGI*, No. 1532, 2–24 (1973).
2. Yu. F. Zhuravlev and B. I. Romanovskii, "Deformation of cavity boundaries by gas jet issued inside the cavity," *Tr. TsAGI*, No. 2294, 16–25 (1985).
3. G. V. Logvinovich, *Hydrodynamics of Flows with Free Boundaries* [in Russian], Naukova Dumka, Kiev (1969).
4. E. V. Paryshev, "Some aspect of calculation of unsteady cavitation flows," in: *Hydrodynamics of Developed Cavitation Flows* (collected scientific papers) [in Russian], No. 2644, Central Aerohydrodynamic Institute, Moscow (2003), pp. 75–92.
5. Yu. F. Zhuravlev, "Interaction of gas jets with a cavity," in: *Collected Papers on Problems of Motion of Solids in a Liquid with High Velocities* [in Russian], TsAGI, Moscow (2002), pp. 57–63.